



Spatial rogue waves in the actively Q-switched Nd:YAG laser under low Kerr nonlinearity

ROZA NAVITSKAYA,^{1,2,*}  IHAR STASHKEVICH,¹ STANISLAV DEREVYANKO,²  AND ALINA KARABCHEVSKY² 

¹Faculty of Physics, Belarusian State University, 4 Nezalezhnasti Avenue, 220030 Minsk, Belarus

²School of Electrical and Computer Engineering, Ben Gurion University of the Negev, Beer Sheva, Israel
*r.navitskaya@gmail.com

Abstract: We report the generation of spatial rogue waves in an actively Q-switched Nd:YAG laser. We observed that spatial rogue waves can emerge when the laser operates in a low-power regime below the self-focusing limit, while the lasing takes place at a large number of high-order transverse modes. These results suggest that the main mechanism leading to rogue waves generation is the modal overlap while large Kerr nonlinearity in the cavity is not a necessary factor in the process of spatial rogue waves formation. We have also investigated the spatio-temporal and coherence properties of the observed rogue waves.

© 2022 Optica Publishing Group under the terms of the [Optica Open Access Publishing Agreement](#)

1. Introduction

Spatial rogue waves (RWs), or “hot spots,” represent tightly focused spontaneously formed areas in the transverse cross-section of the beam with peak intensities much higher than the average beam intensity. In extreme cases, the resulting intensities can lead to damage of the laser crystal or optical elements in the cavity [1]. There is still much uncertainty as to the main mechanisms leading to the emergence of spatial rogue waves in lasers. One of the possible candidates is the spontaneous coupling of transverse and/or longitudinal laser modes [1,2]. Another, more often mentioned mechanism is the medium nonlinearity, which usually is a sufficient factor for rogue waves generation in many optical systems [3]. For example, catastrophic self-focusing in Kerr media causes filamentation and the further breakup of the beam, which leads to spatial RWs formation in a bulk medium [4], as well as optical fibers [5]. In lasers, nonlinear dynamics can lead to the formation of spatiotemporal RWs in semiconductor lasers with intracavity saturable absorbers [6] and multiple-solitons in spatiotemporal mode-locked multimode fiber lasers [7]. However, there are examples of purely linear optical systems where RWs generation was observed [8–10], so the exact role of nonlinearity in the process of rogue wave formation still requires further study.

In our previous study [2] we reported the appearance of hot spots in a passively Q-switched solid-state laser system that employed a saturable absorber (SA). We have demonstrated that the hot spots occurred when a large number of high-order cavity modes were present thus emphasizing the role of the spatial effects. However, several open questions remained. In particular, we were not been able to rule out the effect of the nonlinearity in a passive SA or the Kerr effect in a laser crystal. Moreover, it was not clear whether spatial coherence played a crucial part in the formation of spatial RWs (hot spots). Also, no study of the dynamics of RW pulses was performed.

Therefore, to elucidate these points in our current work we present an experimental study of spatial RWs generation in *actively* Q-switched solid-state laser and investigate their spatial coherence. We show that spatial RWs can be observed in the low-power regime of laser generation when Kerr nonlinearity is negligible while the active Q-switch is purely linear. In addition, we demonstrate that spatial RWs can have lifetimes of about a few cavity round-trip times, which is shorter than the Q-switched pulse length.

2. Experimental setup

The goal of our experimental research is to study the spatial RWs generation in a laser without a passive saturable absorber and under negligible self-focusing effects in the active medium. As a practical implementation of such a system, we used a Nd:YAG laser operating in the active Q-switch regime with low pump energy. The experimental setup is presented in Fig. 1. This setup represents a modification of the system used in our earlier study of spatial RWs generation in the passively Q-switched Nd:YAG laser [2], but with the passive shutter replaced with an active electro-optic shutter, which allows for eliminating the saturable absorption nonlinearity. The total cavity length was equal to 70 cm, while the cylindrical laser crystal had a length of 10 cm and a radius of 0.25 cm. The reflection coefficient of the output mirror was 63%. The output mirror had a flat surface, while the highly reflective mirror had a spherical surface with a radius of curvature equal to 360 cm. The Nd:YAG laser with flashlamp pumping operated in a pulsed regime with a pulse period of 270 ms and was synchronized with a digital camera that captured an output laser beam transverse profile integrated over the Q-switched pulse duration. This laser exhibited quite a large number of transverse lasing modes even for low pump energies, which made it possible to fulfill the main condition required for RWs generation - obtain output laser beams formed by the large number of high-order modes present in the cavity [2]. To control the transverse mode configuration and adjust it to obtain RWs formation, we tuned the laser mirrors and placed an iris diaphragm in the cavity with the same size for all experiments.

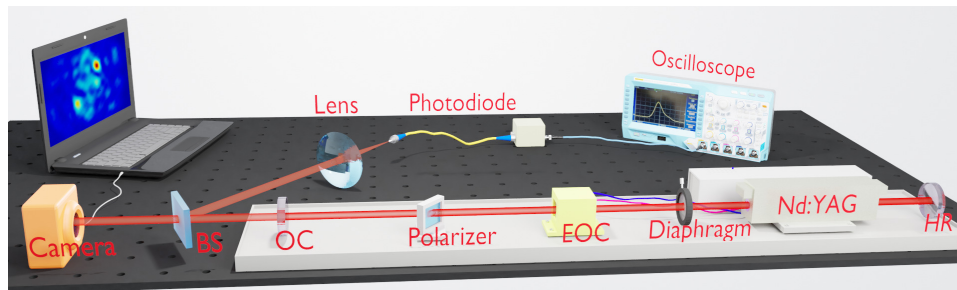


Fig. 1. Schematics of the experimental setup consisting of the following elements: Nd:YAG, laser active element with lamp pumping; HR, highly reflective mirror; iris diaphragm to control the beam size; EOC, electrooptic shutter; polarizer; OC, output coupler; BS, beam splitter; camera connected to the computer to register the transverse profile of the output laser beam; lens; photodiode; oscilloscope to display the temporal intensity profile of the Q-switched pulse.

Nonlinear effects that can potentially be important for RWs generation in the constructed setup are self-focusing in Kerr media, thermal nonlinearity, and nonlinear gain competition in the active medium. While the latter cannot be removed as long as a laser system is considered under study, the former two can be considerably reduced by using low pump powers. To see if there is any effect of increasing Kerr nonlinearity on the process of RWs formation, we performed a number of experiments for several pump energies from relatively high to low (10, 8, and 7 Joules respectively). The minimal energy required for lasing in the Q-switched regime was experimentally found to be 5 J. Typical values of Q-switched pulse parameters such as output pulse energy, FWHM duration, output peak power, and peak power in the cavity for each of these pump energies are summarized in Table 1. The output pulse energy for 10 J was about two times higher than for 7 J, while the peak power was about four times higher. Minimal power required for self-focusing of a Gaussian beam in Nd:YAG (when self-focusing compensates diffraction divergence) is 1.4 MW (Chapter 4 in [11]), which is about 3 times higher than the typical peak power in the cavity for pump energy of 7 J and comparable to the typical peak powers for 8

J and 10 J. For maximal peak power in the cavity (1.99 MW for 10 J pump) and beam waist radius of 1.5 mm the self-focusing length in Nd:YAG is 10.6 m. Thus, our experimental regime corresponded to sub-threshold values for self-focusing for the lowest pump energy of 7 J while its effect increases for 8 J and can become significant for 10 J. This indicates that Kerr nonlinearity in the laser crystal could be a potentially relevant nonlinear mechanism for RWs generation in our setup.

Table 1. Output Q-switched pulse energy, FWHM duration, output peak power, and peak power in the cavity.

E_{pump} , J	E_{pulse} , mJ	T_{FWHM} , ns	P_{peak}^{out} , MW	P_{peak}^{cav} , MW
7	9.40	55.0	0.1709	0.4619
8	14.05	34.0	0.4132	1.1169
10	19.70	26.8	0.7351	1.9867

The strength of thermal effects can be estimated through the average temperature increase of the laser active element after one Q-switched pulse generation. The latter is given by $\Delta T = \eta_h E_{pulse} / CV\rho$, where η_h defines the ratio of the heat load to the output pulse energy and is approximately equal to 3 for a laser with flashlamp pumping [11]. For maximal pump energy used in the experiment, the bulk temperature increase of Nd:YAG laser crystal after one pump cycle was estimated as 0.011 K, and the corresponding refractive index change calculated as $\Delta n = (dn/dT)\Delta T$ is $8.2 \cdot 10^{-8}$. These are quite low values indicating that the effect of thermal nonlinearity in the process of a single Q-switched pulse generation can be neglected in our setup.

3. Results

To investigate whether Kerr nonlinearity affects the properties of spatial RWs under low pulse powers, we performed measurements of the output beam fluctuations from one Q-switched pulse to another for pump energies from 7 to 10 J that correspond to a 4-fold increase in the output pulse peak power. When the pump energy was changed, the configuration of the laser mirrors was adjusted to obtain the most diverse transverse multi-mode generation regime corresponding to large fluctuations of intensity in the profile, while the size of the laser beam was limited by the diaphragm and kept constant for all pump energies. Despite low values of the output peak power which was significantly below the beam self-focusing threshold we were able to observe spatial RWs for pump energy 7 J, as well as for 8 J and 10 J pump energies that corresponded to the increased effect of Kerr nonlinearity. These are shown in Fig. 2(a), Fig. 3(a), and Fig. 4(a) respectively. The right columns in each figure show the observed beam profiles where the spatial RWs did occur while the 1st and 2nd columns correspond to beam profiles without RWs. To determine the rogue wave limit for each experiment, intensity statistics over a number of typical 2D transverse beam profiles was analyzed as shown in Fig. 2(b), Fig. 3(b), Fig. 4(b) along with the calculated values of kurtosis K . For all experiments, the values of kurtosis are larger than 13, which emphasizes a clear L-shaped form of the PDFs and confirms that observed hot spots fulfill the RWs criteria. Background values (intensity lower than $0.1 \langle I_{max} \rangle$) were discarded from the statistics. The rogue wave limit was determined using a standard definition (see e.g. [12]) which defines a RW as a wave with an amplitude exceeding twice the significant wave height (the average of the highest one-third of the amplitudes). In each experiment, we analyzed about 10,000 output pulses to calculate the probability of a Q-switch pulse generation with a spatial RW, which was found to be 0.37%, 0.79%, 0.26% for 7, 8, and 10 J pump energies respectively.

One can see that there are only minor differences between the spatial RWs obtained in all three experiments with different pump energies: peak intensity relative to the average is about 8-8.5 for all regimes, the probabilities of RWs generation are comparable (from 0.3 to less than 1%), the values of kurtosis for intensity PDFs are from 13 to 16, and the sizes of “hot

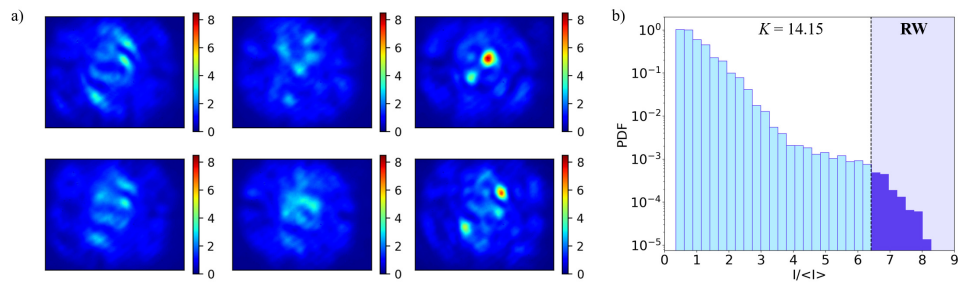


Fig. 2. Generation of spatial rogue waves for 7 J pump energy: (a) typical output laser beam profiles without RWs (1st and 2nd columns) and with RWs (3rd column) (intensity is normalized to its average level); (b) distribution of intensities over a number of 2D transverse beam profiles, the rogue wave limit shown as a boundary of the shaded region, also shown is the value of kurtosis K . The RW limit in Fig. 2(b) corresponds to the relative intensity of 6.41.

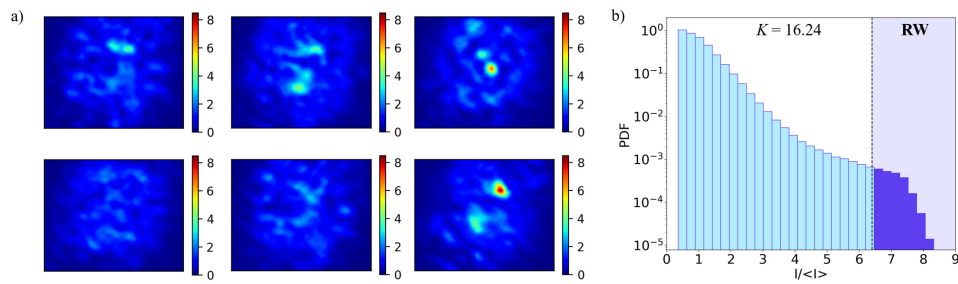


Fig. 3. Same as in Fig. 2 but for 8 J pump energy. The RW limit in Fig. 3(b) corresponds to the relative intensity of 6.40.

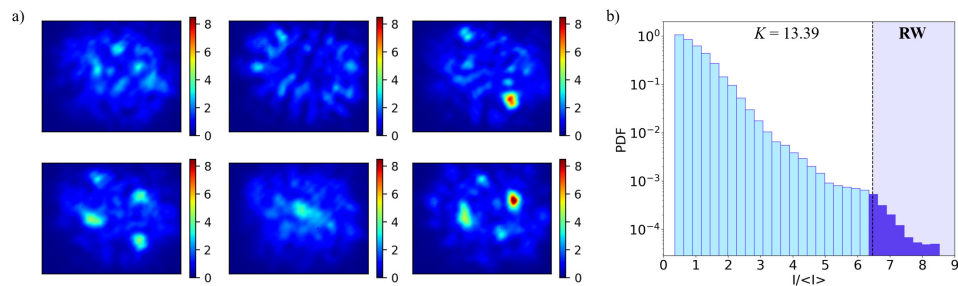


Fig. 4. Same as in Fig. 2 for 10 J pump energy. The RW limit in Fig. 4(b) corresponds to relative intensity of 6.46.

spots” are also close to each other. These results indicate that Kerr nonlinearity does not really affect the RWs generation in low-power regimes below or near the self-focusing limit when the beam size is kept the same and thus is not the main mechanism for spatial RWs formation in a Q-switched solid-state laser. Instead, a necessary condition was to obtain the multi-transverse mode generation regime, when the laser exhibited complex and diverse output beam profiles formed by a large number of high-order transverse modes [2]. This condition was easier to fulfill for larger pump energies as in this case the lasing takes place at a larger number of transverse modes, and for pump energies lower than 7 J it was not possible to obtain the proper mode configuration of the laser. This observation corresponds to the condition of inhomogeneity and granularity of the beam profile leading to spatial rogue waves generation similar to that reported in [10] for a linear multimode fiber. We believe that a similar mechanism is at work in our system as it can be seen from Fig. 2(a), Fig. 3(a), Fig. 4(a) that typical beam profiles obtained in all three experiments are not spatially homogeneous and have quite small speckle sizes.

To confirm the importance of the laser mode configuration for spatial RWs emergence, we performed experiments for different diaphragm sizes and alignment of laser mirrors. In the case of the smaller number of lasing modes with lower order compared to configurations shown in Fig. 2(a), Fig. 3(a), Fig. 4(a) RWs were not observed. Such configuration is shown for example in Fig. 5. Although there are beam profiles with hot spots, their intensities are lower than the RW limit and the kurtosis of the intensity distribution is much smaller than for distributions with RWs.

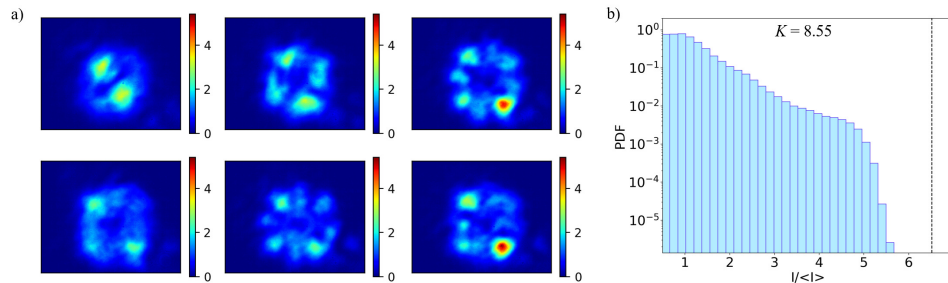


Fig. 5. Same as in Fig. 2 for 10 J pump energy for smaller number of lasing modes and their lower order. The RW limit in Fig. 5(b) corresponds to relative intensity of 6.51.

In addition, in our experiments we analyzed the captured beam profiles to investigate the correlation between the maximal intensity over the transverse distribution and total energy integrated over the beam profile which is equivalent to the total energy of a Q-switched pulse integrated over time. The dependence of total energy normalized to its mean value on the maximal intensity normalized to rogue wave limit for all 3 experiments is shown in Fig. 6 as a scatter plot. We have also calculated the correlation coefficients and these were found to be less than 0.35 which demonstrates a relatively minor correlation between the peak intensities of hot spots and total energy. Fig. 6(b) shows the dependence of the average total energy on pump energy for beam configurations with and without RWs. It is seen that the average total energy for RWs is approximately the same as for beam configurations without RWs. This indicates that spatial RWs are created not due to an increase in total energy of the output pulse, but rather due to energy redistribution between the modes.

The relationship between the spatial and temporal RWs remains one of the interesting questions for future study [6,13,14]. In view of this, we performed experiments to investigate the dynamics of spatial RWs and check whether they exist during an entire Q-switched pulse or some smaller period of time. To this end, we used a detector consisting of four photodiodes that captured parts of the laser beam divided into four quadrants in the transverse plane (top left, top right, bottom

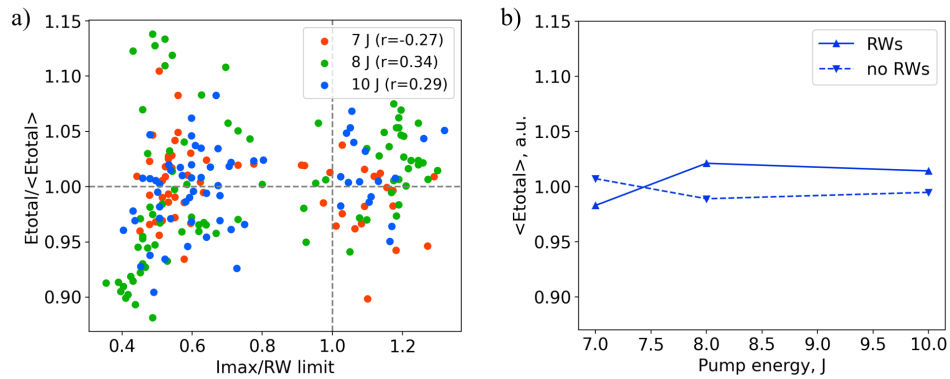


Fig. 6. (a) Dependence of total energy normalized to mean total energy on maximal intensity normalized to rogue wave limit for pump energies of 7, 8, and 10 J. The values of correlation coefficients r are indicated in brackets. (b) Dependence of average total energy on pump energy with and without RWs.

right, bottom left marked with red, blue, green, and yellow colors in Fig. 7). This allows for observing four separate time profiles of Q-switched pulses that correspond to different areas in the laser beam, one of which may contain a spatial rogue wave. Figs. 7(a)-(c) show examples of laser beams with spatial RWs that are located in the bottom right quadrants and correspond to Q-switched pulses under green traces, while Fig. 7(d) shows a laser beam profile without RWs but with well-developed speckle structure. In all cases, the Q-switched pulses corresponding to different areas of the beam have different time profiles with peaks that can be shifted in time or even anti-symmetrical relative to each other. This is seen, for example, by comparing green and yellow traces in Figs. 7(b),(c) that correspond to two different hot spots. In addition, the duration of separate peaks can be of about 10-15 ns (equal to the time of 2-3 cavity round trips, the round trip time $T_c = 5.2$ ns), which is seen in Figs. 7(b)-(d). This indicates that the lifetime of individual speckles and spatial RWs can be in the order of a few round trips, which is smaller than the entire Q-switched pulse duration, and the spatial profile of the laser beam is not static. Furthermore, the pulse shapes under the green traces that correspond to spatial RWs are not smooth and exhibit oscillations with a period of T_c or $2T_c$, which is especially pronounced in Fig. 7(a). This feature indicates that a spatiotemporal mode-locking may take place during the RW generation. We were not able to measure exactly the duration of the laser pulse in the cavity due to the insufficient resolution time of the photodetectors, so this remains one of the questions for future study.

Finally, another interesting question for investigation concerns the coherence properties of the output laser beams. Is spatial coherence a necessary condition for RWs formation? To test this conjecture we built a setup based on a Mach-Zender interferometer (similar to the one proposed in [13]) shown in Fig. 8. The output laser beam was split into two parts: in the first arm of the interferometer, the whole beam with reduced power was transmitted, while in the second arm the beam was magnified with a lens and a small area was selected using a diaphragm. This was needed to ensure high spatial coherence of the reference beam in the second arm of the interferometer. Next, both beams with approximately equal sizes were combined at the CCD camera facet and the presence of the interference fringes was checked which would signify spatially coherent regions of the beam.

Fig. 9 shows interference fringes in the region of spatial RWs captured for the same laser configuration but different Q-switched pulses for pump energy of 8 J. Note that in this experiment, the laser mode configuration differs from the one reported in Fig. 3. The intensity of the reference

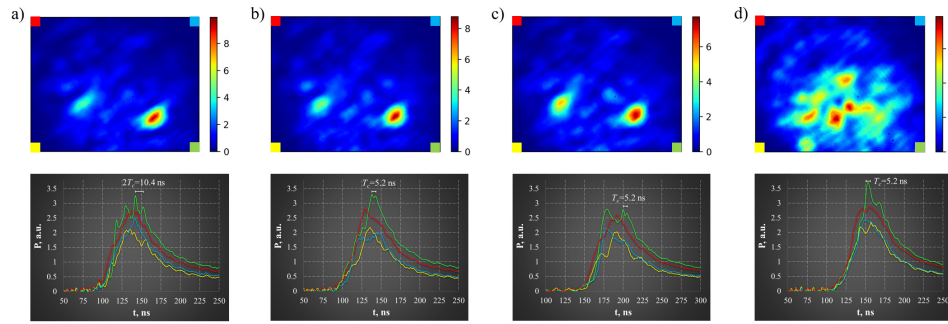


Fig. 7. Laser beam profiles observed for 8 J pump energy and Q-switched pulses measured by four independent photodetectors corresponding to four quadrants in the transverse plane (top left, top right, bottom right, bottom left marked with red, blue, green, and yellow colors): (a)-(c) spatial RW in the bottom right quadrant (corresponds to the Q-switched pulse defined by a green trace); (d) no RWs, a well-developed speckle pattern. The cavity round-trip time T_c is indicated in the bottom plots.

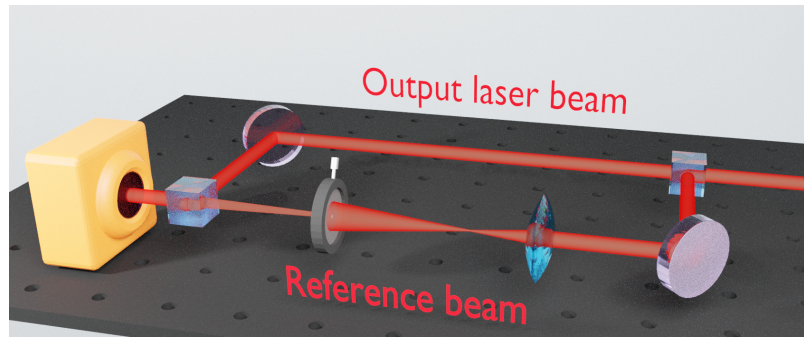


Fig. 8. Scheme of the Mach-Zender interferometer setup used to measure the spatial coherence of the output laser beam.

beam in the second channel was about 10 times lower than the peak intensity of the laser beam in the first channel. Maximal possible visibility of the interference pattern for such conditions ($I_2 = 0.1I_1$) is equal to $V = 2\sqrt{I_1I_2}/(I_1 + I_2) = 0.575$. It is seen that for one output beam (Fig. 9(a)) there are high contrast fringes in the region of RW corresponding to high spatial coherence (visibility in the “hot spot” region is 0.16, maximal visibility over the beam profile is 0.32), while for the other output beam (Fig. 9(b)) the fringes in the region of RW are almost absent indicating low spatial coherence (visibility in the RW region is 0.037, maximal visibility over the beam profile is 0.34). Both output beams were captured for the same position of the diaphragm selecting the reference beam. Low visibility of the interference pattern could be explained by low temporal coherence between the hot spot and reference beam, which happens when these regions of the beam exist in different moments of time like in Fig. 7(c). However, RWs with high spatial coherence were observed in the majority of cases. These results suggest that usually transverse modes combine coherently to form a spatial rogue wave.

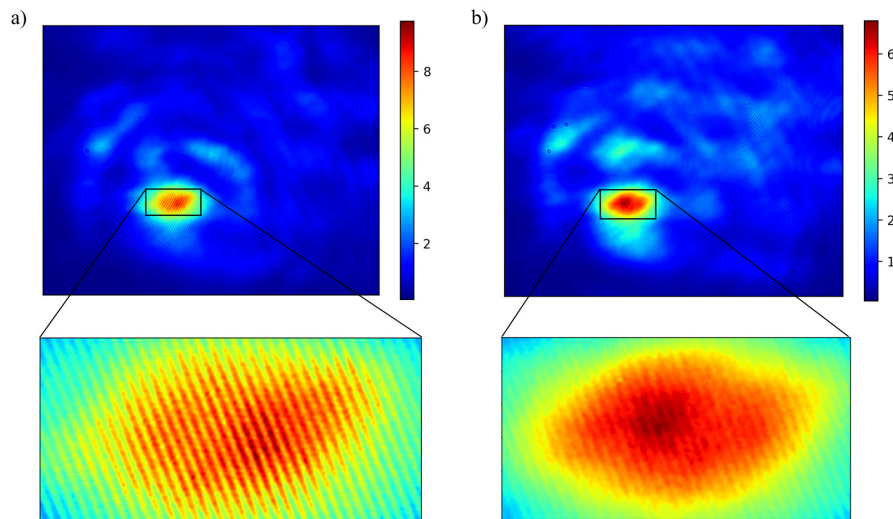


Fig. 9. Example rogue waves with (a) high and (b) low spatial coherence for the same laser configuration.

4. Conclusions

To conclude, we demonstrated the experimental generation of spatial rogue waves in the actively Q-switched solid-state laser operating in a low-power regime below the self-focusing limit. The obtained results confirm that large Kerr nonlinearity causing self-focusing in the cavity is not necessary for the spatial RWs to emerge, while the presence of a large number of high-order transverse modes is critical. We have also demonstrated that there is little correlation between the maximum intensity of a hot spot and the total Q-switched pulse energy. Furthermore, spatial RWs can correspond to Q-switched pulses with oscillatory structure characteristic to mode-locking generation, and the lifetimes of individual hot spots can be smaller than the entire Q-switched pulse length. These results are important for future studies of the role of nonlinearity and spatial effects in the process of spatial rogue waves formation in lasers.

Funding. Israel Science Foundation (2598/20); Belarusian Republican Foundation for Fundamental Research (F211ZR-005).

Disclosures. The authors declare no conflicts of interest.

Data availability. Data underlying the results presented in this paper are not publicly available at this time but may be obtained from the authors upon reasonable request.

References

1. G. Arisholm, "Self-focusing and optical damage in a diode-pumped neodymium laser," *OSA TOPS, Vol. 10, Advanced Solid State Lasers* (Optical Society of America, 1997), p. 109.
2. R. Navitskaya, I. Stashkevich, S. Derevyanko, and A. Karabchevsky, "Experimental demonstration of spatial rogue waves in the passively q-switched nd:yag laser," *Opt. Lett.* **46**(15), 3773–3776 (2021).
3. N. Akhmediev, B. Kibler, and F. Baronio, *et al.*, "Roadmap on optical rogue waves and extreme events," *J. Opt.* **18**(6), 063001 (2016).
4. T. Hansson, D. Anderson, M. Desaix, and M. Lisak, "Self-similar collapse and blow up of laser beams in nonlinear Kerr media-revisited," *Opt. Commun.* **284**(13), 3422–3427 (2011).
5. P. M. Lushnikov and N. Vladimirova, "Non-gaussian statistics of multiple filamentation," *Opt. Lett.* **35**(12), 1965 (2010).
6. S. Coulbaly, M. G. Clerc, F. Selmi, and S. Barbay, "Extreme events following bifurcation to spatiotemporal chaos in a spatially extended microcavity laser," *Phys. Rev. A* **95**(2), 023816 (2017).
7. Y. Ding, X. Xiao, P. Wang, and C. Yang, "Multiple-soliton in spatiotemporal mode-locked multimode fiber lasers," *Opt. Express* **27**(8), 11435 (2019).

8. C. Liu, R. E. C. van der Wel, N. Rotenberg, L. Kuipers, T. F. Krauss, A. D. Falco, and A. Fratalocchi, "Triggering extreme events at the nanoscale in photonic seas," *Nat. Phys.* **11**(4), 358–363 (2015).
9. C. Bonatto, S. D. Prado, F. L. Metz, J. R. Schoffen, R. R. B. Correia, and J. M. Hickmann, "Super rogue wave generation in the linear regime," *Phys. Rev. E* **102**(5), 052219 (2020).
10. F. Arecchi, U. Bortolozzo, A. Montina, and S. Residori, "Granularity and inhomogeneity are the joint generators of optical rogue waves," *Phys. Rev. Lett.* **106**(15), 153901 (2011).
11. W. Koechner, *Solid-State Laser Engineering* (Springer, 2006).
12. J. M. Dudley, G. Genty, A. Mussot, A. Chabchoub, and F. Dias, "Rogue waves and analogies in optics and oceanography," *Nat. Rev. Phys.* **1**(11), 675–689 (2019).
13. C. R. Bonazzola, A. A. Hnilo, M. G. Kovalsky, and J. R. Tredicce, "Features of the extreme events observed in the all-solid state laser with a saturable absorber," *Phys. Rev. A* **92**(5), 053816 (2015).
14. C. Bonazzola, A. Hnilo, M. Kovalsky, and J. Tredicce, "Extreme events and single-pulse spatial patterns observed in a self-pulsing all-solid-state laser," *Phys. Rev. E* **97**(3), 032215 (2018).